

Final Draft
of the original manuscript:

Sharp, M.; Pranzas, K.; Schreyer, A.:

**Going Ultra: How We Can Increase the Length Scales Studied in
Small-Angle Neutron Scattering**

In: Advanced Engineering Materials (2009) Wiley

DOI: 10.1002/adem.200800331

Going Ultra: How we can increase the length scales studied in small-angle neutron scattering

Melissa A. Sharp, P. Klaus Pranzas and Andreas Schreyer

Institute for Materials Research, Geesthacht Neutron Facility, GKSS Research Centre,
Max-Planck Strasse 1, 21502 Geesthacht, Germany

Email: melissa.sharp@gkss.de

Abstract

Small-angle neutron scattering has over the years proved to be a popular technique to investigate a variety of problems in materials science, since the length scales probed by this technique (1-100 nm) are ideal for many systems. However, there are a number of problems where the length scale of interest is larger. In order to study such systems it is possible to combine small-angle neutron scattering (SANS) with ultra-small-angle neutron scattering (USANS). This allows the study of structures from a few nanometres up to 50 μm . Here it is shown how the combination of SANS and USANS has allowed for a wider range of problems within materials science and polymer science to be solved.

1 Introduction

Small-angle neutron scattering (SANS) has in recent years become an extremely popular technique for investigating materials on the nanometre scale. There are several reasons for this: The length scales that can be probed with this technique are ideal for many materials investigations (the sizes that can be probed are typically 1 - 100 nm) and the information obtained is an average over the whole sample. In addition the measurements are relatively simple to carry out and in most cases no additional sample preparation is necessary. Moreover, contrast matching has proved an invaluable tool in investigating the detailed structure of materials, particularly within soft matter research. However, many materials also contain important and interesting features on larger length scales than those that can be probed with conventional pinhole SANS instruments. In this case the ultra-small angle neutron scattering (USANS) technique becomes useful. USANS extends the size range studied by some orders of magnitude, allowing for the investigation of structural features from the nanometre scale up to 50 μm .

This article aims to show how we can get additional important information about materials by employing the USANS technique in addition to the information obtained by SANS measurements. Two examples shall be given: One involving polymeric micelles and the other hydrogen storage materials. These examples focus on work carried out at the Geesthacht Neutron Facility (GeNF), and the article will therefore begin with a brief overview of the SANS and USANS instruments at GeNF.

2 The instruments

At GeNF the neutrons are produced from the research reactor FRG-1, which is equipped with a cold source, to which the small-angle instruments are connected. The SANS-2

instrument at GeNF is a conventional pinhole small-angle scattering diffractometer,^[1,2] as shown in Figure 1. Some of the important features of the instrument are listed in Table 1; further information can be found on the Internet at <http://genf.gkss.de>. The instrument employs a velocity selector and up to 16 m collimation can be used. A two-dimensional movable area detector is used, allowing both isotropic and anisotropic scattering to be measured. The Double Crystal Diffractometer (DCD) at GeNF uses a Bonse-Hart type setup^[3] and is illustrated in Figure 2. Some of the important characteristics of the instrument are listed in Table 1. The instrument has previously been described by Bellmann *et al.*^[4,5] It consists of triple-bounce channel-cut perfect Si(111) crystals. The monochromator crystal is aligned to maximise the flux reaching the sample. The analyser crystal is rotated during the measurement to measure the scattering from all angles of interest. The instrument employs one-dimensional ³He detectors. It is possible to achieve a good overlap of the Q -range of these two instruments, allowing the measurement of samples in the Q -range $1 \times 10^{-4} - 3 \text{ nm}^{-1}$. A number of sample environments are available which may be used at both the SANS-2 and DCD instruments; these are listed in Table 2.

Since the scattering data obtained from the DCD instrument is slit-smeared,^[6] it is necessary to be able correct for this, if the data obtained at DCD is to be successfully combined with the scattering curves measured at SANS-2. In addition multiple-scattering effects often play a significant role when measuring the scattering of large structures. Both of these effects can be corrected for during the data reduction procedure used to treat data obtained at the DCD instrument.^[7]

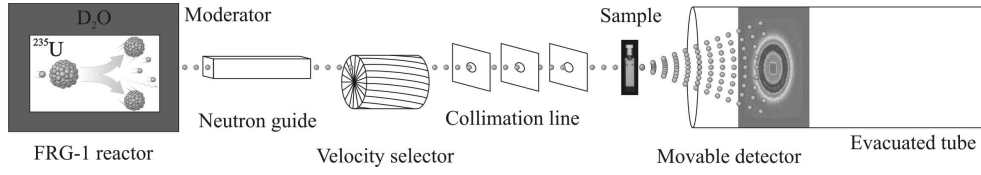


Figure 1: The SANS-2 instrument at GeNF

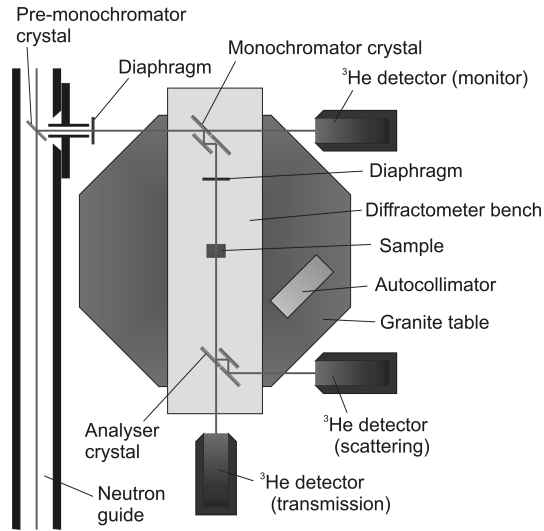


Figure 2: The Double Crystal Diffractometer at GeNF

	SANS-2	DCD
Deflecting crystal	—	Si(111)
Monochromator	helical slot velocity selector	channel-cut perfect Si crystals, triple-bounce
Detectors	2-dimensional position sensitive ^3He detector, 2 mm resolution	3 ^3He detectors
Wavelengths	0.3 - 2.0 nm	0.443 nm
Wavelength dispersion	$\Delta\lambda/\lambda = 0.1$	$\Delta\lambda/\lambda = 1 \times 10^{-5}$
Angular resolution	—	$< 0.05\mu\text{rad}$
Flux at sample position	$2 \times 10^7 \text{ n cm}^{-2} \text{ s}^{-1}$	$550 \text{ n cm}^{-2} \text{ s}^{-1}$
Q -range	$1 \times 10^{-2} - 3 \text{ nm}^{-1}$	$1 \times 10^{-4} - 5 \times 10^{-2} \text{ nm}^{-1}$

Table 1: Instrument specifics for SANS-2 and DCD

Sample environment	Specifications
Sample changer	6 positions
Sample changer with heater	Temperature range 5 – 80°C, 5 positions
Electromagnet	Vertical field, ≤ 0.9 T
Rotating rack	3 positions, for unstable dispersions

Table 2: Sample environments that can be used on both DCD and SANS-2

3 Applications

Ultra-small-angle neutron scattering measurements have been applied in many areas of science, from materials science,^[8–10] the investigation of porous and fractal systems,^[11–13] biomaterials research,^[14, 15] colloidal particles and crystals^[16–18] to polymer science.^[19–22] Two examples of recent work carried out using both SANS and USANS shall be discussed next. The examples, one involving polymeric micelles, the other hydrogen storage materials, illustrate how ultra-small-angle neutron scattering measurements have been able to give significant further information compared to the small-angle neutron scattering measurements alone.

3.1 Polymeric micelles

Block copolymers may form micelles when placed in certain solvents, depending on the interaction of the different blocks with the solvent. Such micelles are interesting since they can potentially be used as drug delivery agents.^[23–26] As part of an investigation into the effect of various model adjuvants on the structure of polymeric micelles, some interesting changes were observed in the low- Q part of the SANS scattering curves for the maximum amount of adjuvant soluble, as the temperature was increased.^[27] The polymers used in this investigation were Pluronic block copolymers, of structure poly(ethylene oxide)-*b*-poly(propylene oxide)-*b*-poly(ethylene oxide). The model adju-

vant with which this effect was observed was benzyl alcohol. Figure 3 shows the SANS curves obtained for 10 wt % Pluronic P105 with 7 wt % benzyl alcohol added as the temperature is increased from room temperature to body temperature; these data were obtained on the LOQ (SANS) instrument at the ISIS Pulsed Neutron and Muon Source, UK. It can be seen that in the low- Q part of the curve there is an increase in the scattering intensity as the temperature is increased. However, the origin of this effect cannot be determined from these scattering curves alone. Two potential scenarios seem reasonable: It might arise from a change in the shape of the micelles from spheres to rods. Such changes have been reported for related systems.^[28-30] However, since the changes in the scattering curves only affect the part of the scattering curve dominated by the intermicellar interactions, another reasonable explanation is that there is a change in the interaction potential between the micelles. In order to determine which of these explanations seems the most reasonable, USANS measurements were carried out. This was done on the DCD instrument at GeNF. The desmeared scattering curve obtained is shown in Figure 4, together with the SANS data. There is a gap between the SANS and USANS curves, arising from the Q -range available with the instruments used for the measurements - the lowest Q that could be reached on the LOQ instrument was 0.09 nm^{-1} , which unfortunately is not low enough to allow for an overlap with the USANS data obtained on the DCD instrument. What can be observed is a Q^{-4} dependency in the high- Q region ($0.25 - 0.8 \text{ nm}^{-1}$) and in the low- Q region ($1 \times 10^{-3} - 3 \times 10^{-3} \text{ nm}^{-1}$). In the intermediate part of the scattering curve a Q -dependency of exponent $-1.7 - -2.2$ is seen. The slight discrepancy between the Q -dependency of the SANS and USANS curves in this region is attributed to slight differences in sample composition and temperatures. The results can be interpreted as follows: The Q^{-4} dependency in the high- Q part corresponds to Porod scattering of the micelles. The intermediate part of the scattering curve, which has an approximate Q^{-2} -dependence over more than an

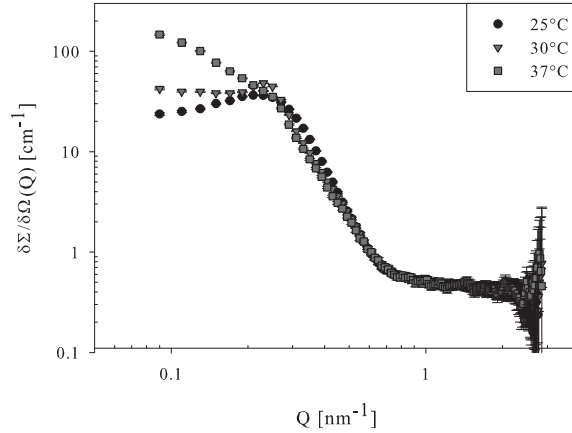


Figure 3: Effect of temperature on 10 wt % Pluronic P105 with 7 wt % benzyl alcohol, where benzyl alcohol has been matched to the aqueous solution. It can be seen that as the temperature is increased, the scattering in the low- Q part of the scattering curve begins to increase.

order of magnitude, comes from the scattering of a mass fractal system. This is thought to arise from the micelles aggregating into larger agglomerates, which show mass fractal characteristics. The Q^{-4} dependency in the low- Q part is the Porod scattering from these larger agglomerates. In other words, the combined SANS and USANS observations support the explanation that there is a change in the intermicellar interaction potential. At lower temperatures the micelles have a repulsive interaction potential, while as the temperature is increased this changes to an attractive interaction potential, leading the micelles to form larger agglomerates with mass fractal characteristics. This is illustrated in Figure 5.

3.2 Hydrogen storage materials

Hydrogen is thought to be one of the important alternative fuels for the future, in particular it could be used as a zero-emission vehicle fuel. At GKSS Research Centre there is a focus on the development and optimisation of light metal hydrides for stor-

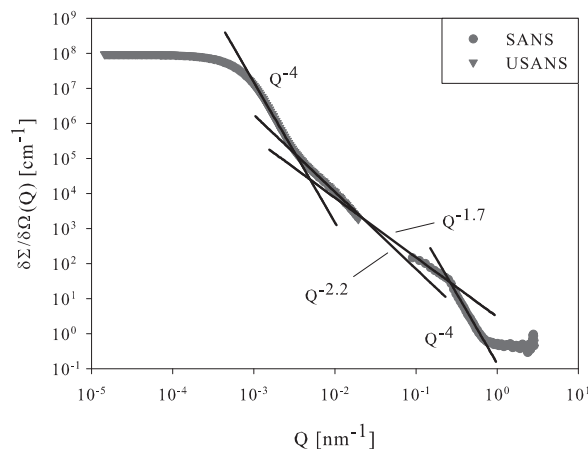


Figure 4: 10 wt % Pluronic P105 with 7 wt % benzyl alcohol at 37°C, where benzyl alcohol has been matched to the aqueous solution. Shown are both the SANS and USANS scattering curves. Also shown are the Q -dependencies matching different parts of the scattering curves.

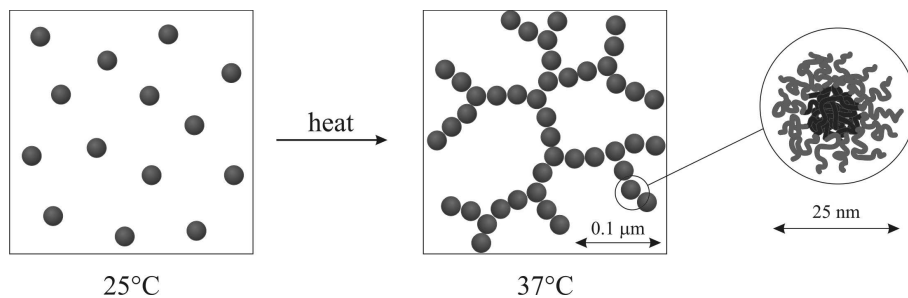


Figure 5: Illustration of the change in interaction potential as the micelles are heated. At room temperature the interaction potential is repulsive, while it becomes attractive as the sample is heated, leading to the micelles to form agglomerates with mass fractal characteristics.

ing hydrogen,^[31–33] since they offer a good and safe alternative for hydrogen storage compared to compressed or liquid hydrogen. It has been found that nanocrystalline magnesium hydride has a high storage capacity (up to 7.6 wt %), while the absorption and desorption rates of hydrogen are improved significantly by the addition of metal oxide catalysts.^[31,32,34] However, relatively little work had until recently been carried out to understand the structural changes that take place during the absorption and desorption of hydrogen. Measurements were therefore carried out on the SANS-2 and DCD instruments at GeNF on samples of magnesium hydride produced using the high-energy ball milling technique.^[35] The combined scattering curves from the two instruments are shown in Figure 6; it can clearly be seen that a good overlap is achieved between these two instruments. For clarity only two scattering curves are shown here: firstly of the magnesium hydride in the as-milled state and secondly the magnesium hydride after two cycles of absorption and desorption; details of further measurements can be found in Pranzas *et al.*^[35] Using a model of hard spheres a size distribution was obtained for these samples, the results of which are also shown in Figure 6. The results show the presence of large magnesium hydride powder particles in the size range 500 nm - 20 μm . In addition nanocrystallites of magnesium hydride with sizes of the order of magnitude 4-6 nm are present. It was found that as hydrogen is absorbed and desorbed there is a shift for the nanocrystallites to larger sizes, as well as a broadening of the size distribution. At the same time it can be observed that the powder particles decrease in size. In other words, there is a coarsening of the nanocrystallites taking place, while the larger powder particles begin to break up into smaller particles; this is illustrated in Figure 7.

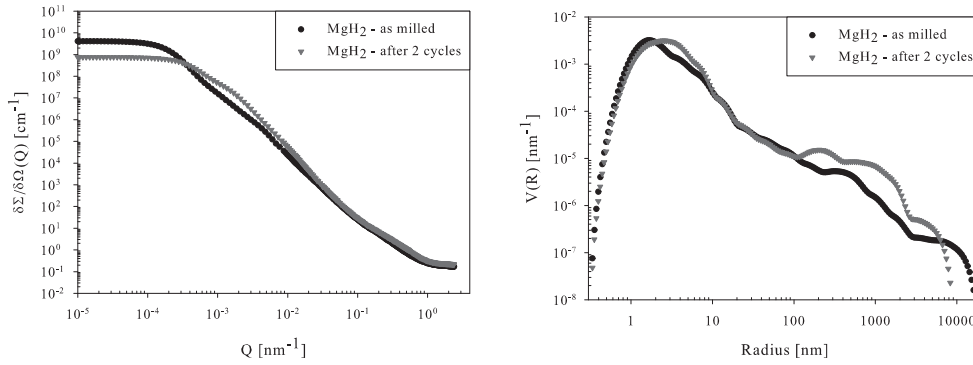


Figure 6: Scattering curves obtained from SANS and USANS measurements of magnesium hydride in the as-milled state and after two cycles of loading/unloading of hydrogen (left). Also shown are the size distributions obtained when fitting the scattering curves to a hard sphere model (right).

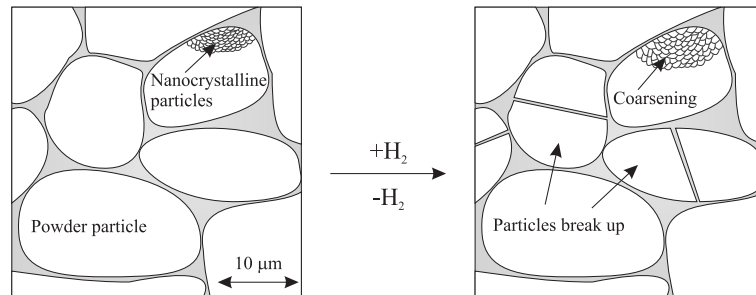


Figure 7: As hydrogen is loaded and unloaded the magnesium hydride powder particles begin to break up, while there is a coarsening of the nanocrystallites.

4 Conclusions

Ultra-small-angle neutron scattering is a powerful tool that can complement SANS measurements when it comes to investigating the structure of materials. It extends the size range that can be investigated significantly, from 100 nm to more than 30 μm . In this article it has been shown how combining SANS and USANS measurements has been able to provide significant additional information on two important systems in polymer and materials science. The combined techniques clearly have a large potential in many areas of science and will ultimately benefit the scientific community.

Acknowledgements

We thank ISIS for the provision of neutron beamtime, in particular Stephen King for his assistance during the measurements. We would like to thank Terence Cosgrove, Peter Staron, Dieter Bellmann, Martin Dornheim and K.F. Aguey-Zinsou for sample preparation and helpful discussions. BASF are gratefully acknowledged for supply of the Pluronic polymers. MAS acknowledges AstraZeneca and EPSRC for funding of her doctoral work.

References

- [1] S. King, In *Modern techniques for polymer characterisation* (Eds: R. Pethrick, J. Dawkins), John Wiley Sons Ltd, **1999**, Ch. 7.
- [2] J. Higgins, H. Benoit, *Polymers and neutron scattering*, Oxford Series on Neutron Scattering in Condensed Matter; Oxford University Press, **1996**.
- [3] U. Bonse, M. Hart, *Appl. Phys. Lett.* **1965**, 7, 238.

- [4] D. Bellmann, M. Klatt, R. Kampmann, R. Wagner, *Physica B* **1998**, 241-243, 71.
- [5] D. Bellmann, P. Staron, P. Becker, *Physica B* **2000**, 276-278, 124.
- [6] R. Roe, *Methods of X-ray and Neutron Scattering in Polymer Science*; Oxford University Press, **2000**.
- [7] P. Staron, D. Bellmann, *J. Appl. Crystallogr.* **2002**, 35, 75.
- [8] C. Buckley, H. Birnbaum, D. Bellmann, P. Staron, *J. Alloys Compd.* **1999**, 293-295, 231.
- [9] P. Staron, D. Bellmann, R. Kampmann, M. Klatt, R. Wagner, *Physica B* **1998**, 241-243, 98.
- [10] V. Wagner, D. Bellmann, *Physica B* **2007**, 397, 27.
- [11] A. Radlinski, E. Radlinska, M. Agamalian, G. Wignall, P. Lindner, O. Randl, *Phys. Rev. Lett.* **1999**, 82, 3078.
- [12] F. Triolo, A. Triolo, M. Agamalian, J. Lin, R. Heenan, G. Lucido, R. Triolo, *J. Appl. Crystallogr.* **2000**, 33, 863.
- [13] D. Bellmann, H. Clemens, J. Banhart, *Appl. Phys. A* **2002**, 74, S1136.
- [14] H. Tanaka, S. Koizumi, T. Hashimoto, K. Kurosaki, S. Kobayashi, *Macromolecules* **2007**, 40, 6304.
- [15] S. Koizumi, Z. Yue, Y. Tomita, T. Kondo, H. Iwase, D. Yamaguchi, T. Hashimoto, *Eur. Phys. J. E* **2008**, 26, 137.
- [16] H. Matsuoka, T. Ikeda, H. Yamaoka, M. Hashimoto, T. Takahashi, M. Agamalian, G. Wignall, *Langmuir* **1999**, 15, 293.

- [17] C. Muzny, B. Butler, H. Hanley, M. Agamalian, *J. Phys.: Condens. Matter* **1999**, *11*, L295.
- [18] T. Harada, H. Matsuoka, T. Yamamoto, H. Yamaoka, J. Lin, M. Agamalian, G. Wignall, *Colloids Surf., A* **2001**, *190*, 17.
- [19] N. Wanakule, A. Nedoma, M. Robertson, Z. Fang, A. Jackson, B. Garetz, N. Balsara, *Macromolecules* **2008**, *41*, 471.
- [20] V. Ryukhtin, P. Stepanek, Z. Tuzar, K. Pranzas, D. Bellmann, *Physica B* **2006**, *385-286*, 762.
- [21] S. Agrawal, N. Sanabria-DeLong, P. Jemian, G. Tew, S. Bhatia, *Langmuir* **2007**, *23*, 5039.
- [22] M. Agamalian, R. Alamo, M. Kim, J. Londono, L. Mandelkern, G. Wignall, *Macromolecules* **1999**, *32*, 3093.
- [23] M. Malmsten, *Soft Matter* **2006**, *2*, 760.
- [24] N. Rapoport, *Colloids Surf., B* **1999**, *16*, 93.
- [25] C. Allen, D. Maysinger, A. Eisenberg, A. *Colloids Surf. B* **1999**, *16*, 3.
- [26] A. Kabanov, E. Batrakova, V. Alakhov, *J. Controlled Release* **2002**, *82*, 189.
- [27] M. Sharp, *PhD Thesis*, University of Bristol, **2007**.
- [28] K. Mortensen, *J. Phys.: Condens. Matter* **1996**, *8*, A103.
- [29] S. King, R. Heenan, V. Cloke, C. Washington, *Macromolecules* **1997**, *30*, 6215.
- [30] R. Ganguly, V. Aswal, P. Hassan, I. Gopalakrishnan, J. Yakhmi, *J. Phys. Chem. B* **2005**, *109*, 5653.

- [31] W. Oelerich, T. Klassen, R. Bormann, *J. Alloys Compd.* **2001**, 315, 237.
- [32] G. Barkhordarian, T. Klassen, R. Bormann, *Scr. Mater.* **2003**, 49, 213.
- [33] M. Dornheim, N. Eigen, G. Barkhordarian, T. Klassen, R. Bormann, *Adv. Eng. Mater.* **2006**, 8, 377.
- [34] G. Barkhordarian, T. Klassen, R. Bormann, *J. Alloys Compd.* **2004**, 364, 242.
- [35] P. Pranzas, M. Dornheim, D. Bellmann, K. Aguey-Zinsou, T. Klassen, A. Schreyer, *Physica B* **2006**, 385-386, 630.